AD NUMBER

ADB017876

LIMITATION CHANGES

TO:

Approved for public release; distribution is unlimited.

FROM:

Distribution authorized to U.S. Gov't. agencies only; Administrative/Operational Use; MAR 1977. Other requests shall be referred to Department of Defense, Attn: Public Affairs Office, Washington, DC 20301.

AUTHORITY

GE and DoD Notice dtd 14 Dec 1977

THE EFFECT OF TROPOSPHERIC REFRACTION ON HF PROPAGATION

R77EMH5

George H. Millman

March 1977

General Electric Company
Syracuse, New York 13201

GENERAL ELECTRIC COMPANY TECHNICAL INFORMATION

Within the limitations imposed by Government data export regulations and security classifications, the availability of General Electric Company technical information is regulated by the following classifications in order to safeguard proprietary information:

CLASS 1: GENERAL INFORMATION

Available to anyone on request.
Patent, legal and commercial review required before issue.

CLASS 2: GENERAL COMPANY INFORMATION

Available to any General Electric Company employee on request.
Available to any General Electric Subsidiary or Licensee subject to existing agreements.
Disclosure outside General Electric Company requires approval of originating component.

CLASS 3: LIMITED AVAILABILITY INFORMATION

Original Distribution to those individuals with specific need for information.
Subsequent Company availability requires originating component approval.
Disclosure outside General Electric Company requires approval of originating component.

CLASS 4: HIGHLY RESTRICTED DISTRIBUTION

Original distribution to those individuals personally responsible for the Company's interests in the subject.
Copies serially numbered, assigned and recorded by name.
Material content, and knowledge of existence, restricted to copy holder.

GOVERNMENT SECURITY CLASSIFICATIONS, when required, take precedence in the handling of the material. Wherever not specifically disallowed, the General Electric classifications should also be included in order to obtain proper handling routines.

TIS Distribution Center
CSP 4-Lobby, X7712
Syracuse, New York 13201

GENERAL ELECTRIC

HEAVY MILITARY EQUIPMENT DEPARTMENT

(9) TECHNICAL INFORMATION SERIES

Author	Subject Category	(14) No. R77EMH5
(10) G.H. Millman	HF Propagation Tropospheric Refraction	(11) Date Mar 77

Title

(6) THE EFFECT OF TROPOSPHERIC REFRACTION ON HF PROPAGATION

Copies Available at	GE Class 1	No. of Pages
HMED TIS Distribution Center Box 1122 (CSP4-Lobby) Syracuse, New York 13201	Govt Class Unclassified	(12) 54

Summary

An evaluation is made of the effect of refractive bending in the troposphere on the propagation of high frequency (HF) radio waves. The index of refraction in the troposphere is defined in terms of the CRPL Reference Refractivity Atmosphere - 1958. The electron density in the ionosphere is represented by a Chapman model. Ray tracings are performed based on the assumption that the propagation media are stratified into layers of constant refractive index. The ground scatter distance and the true and virtual reflection heights are calculated as a function of surface refractivity and various electron density profiles.

Key Words

Tropospheric Refraction
Ionospheric Refraction
Chapman Model
HF Propagation

Send to

-A-

GENERAL ELECTRIC COMPANY
HEAVY MILITARY EQUIPMENT DEPARTMENT
TECHNICAL INFORMATION SERIES

SECTION Advanced Development Engineering

UNIT 570

HMED ACCOUNTING REFERENCE

COLLABORATORS

APPROVED J.C. Buchta TITLE Mgr., ADE LOCATION CSP 4-58

TIS R77EMH5

MINIMUM DISTRIBUTION - Government Unclassified Material (and Title Pages) in G.E. Classes 1, 2, or 3 will be the following.

Copies	Title Page Only	To
0	1	Legal Section, HMED (Syracuse)
0	1	Manager, Technological Planning, HMED (Syracuse)
5	6	G-E Technical Data Center (Schenectady)

MINIMUM DISTRIBUTION - Government Classified Material, Secret or Confidential in G.E. Classes 1, 2, or 3 will be the following.

1	1	Classified Section, Electronics Park Library
1	0	Manager, Technological Planning, HMED (Syracuse)

ADDITIONAL DISTRIBUTION (Keep at minimum within intent of assigned G.E. Class.)

COPIES	NAME	LOCATION
5	DEFENSE DOCUMENTATION CENTER	CAMERON STATION, ALEXANDRIA, VA. 22314
(CLASS 1 ONLY) 1	L. I. Chasen	P.O. Box 8555 Philadelphia, Pa., 19101

TABLE OF CONTENTS

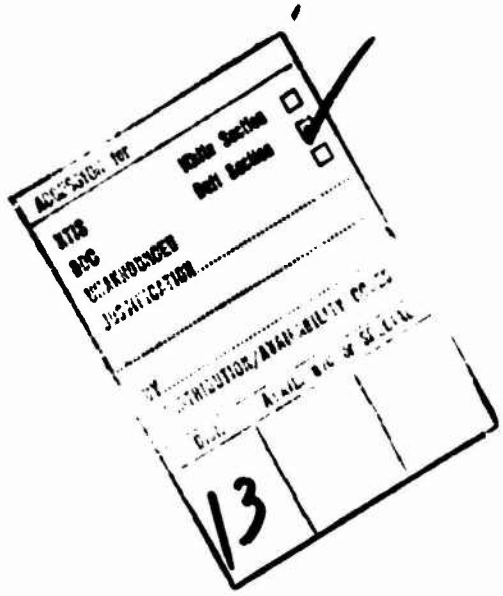

LIST OF ILLUSTRATIONS

LIST OF TABLES

GLOSSARY

C	Coulomb
CRPL	Central Radio Propagation Laboratory
°K	degrees Kelvin
F	Farad
G	Gauss
H	Henry
HF	High Frequency
kg	kilogram
km	kilometer
m	meter
mbar	millibar
MHz	megaHertz
rad	radian
s	second
Wb	Weber

SECTION I

INTRODUCTION

When electromagnetic waves are propagated through the troposphere and ionosphere, they undergo a change in direction or refractive bending. This phenomenon which arises from the nonhomogeneous characteristics of the media introduces an angular error in radar measurement data (Millman, 1958).

The deviation of the elevation angle of radar waves by the troposphere is independent of frequency, and the deviation by the ionosphere is frequency dependent, i.e., inversely proportional to frequency squared (Millman, 1958). However, in the case of the troposphere, the angular deviation is directly proportional to the surface refractivity, N_o, i.e., the deviation increasing with increasing N_o (Millman, 1970).

In predicting the range-coverage performance of an HF backscatter radar or the transmission-frequency requirements of a communications system, ionospheric propagation characteristics are only considered. The effects of the tropospheric refractive properties are in general not taken into account. However, a preliminary examination of the HF propagation phenomena has revealed that the ground scatter distance and the true and virtual reflection heights are modified when tropospheric refraction effects are taken into account (Millman, 1975).

In this report, an estimate is made of the effect of tropospheric refractive bending on the propagation of HF radio waves. The index of refraction in the troposphere is modeled in terms of the CRPL Reference Refractivity Atmosphere - 1958, while the index of refraction in the ionosphere is defined in terms of the transverse-ordinary mode of propagation.

SECTION II

THEORETICAL CONSIDERATIONS

2.1 TROPOSPHERIC INDEX OF REFRACTION

The index of refraction, n, in the troposphere, can be expressed in terms of the functions

$$N = (n - 1) \times 10^6 \tag{2-1}$$

and

$$N = \frac{a}{T} \left(p + \frac{b\epsilon}{T} \right) \tag{2-2}$$

where N is the refractivity, T is the air temperature (°K), p is the total pressure (mbar) and ϵ is the partial pressure of water vapor (mbar). According to Smith and Weintraub (1953), the constants, a and b, are 77.6°K/mbar and 4810°K, respectively.

It should be noted that the above expression for the refractivity of air is independent of frequency in the 100- to 30,000-MHz range. The first term in Equation (2-2), ap/T, applies to both optical and radio frequencies, and is often referred to as the dry term. The second term, $ab\epsilon/T^2$, which is the wet term, is the water vapor relationship required only at radio frequencies.

The tropospheric refractive index model employed in this analysis is the CRPL Reference Refractivity Atmosphere - 1958 (Bean and Dutton, 1966) which is described by

$$N(h) = N_o + (h - h_o) \Delta N \tag{2-3}$$

where $N = (n - 1) \times 10^6$, N_o is the surface refractivity, h_o is the surface height above mean sea level and n is the index of refraction. This expression is valid for $h_o \leq h \leq (h_o + 1)$ km. The parameter, ΔN, is defined by

$$N = -7.32 \exp (0.005577\, N_o) \tag{2-4}$$

For the region defined by $(h_o + 1) \leq h \leq 9$ km, the refractivity decays as

$$N(h) = N_1 \exp [-c (h - h_o - 1)] \tag{2-5}$$

where N_1 is the value of N(h) at 1 km above the surface and

$$c = \frac{1}{8 - h_o} \log_e \left(\frac{N_1}{105}\right) \tag{2-6}$$

Above 9 km, the exponential decay is of the form

$$N(h) = 105 \exp [-0.1424 (h - 9)] \tag{2-7}$$

Surface refractivities of 320-N and 400-N units were only considered. The latter is representative of severe refraction conditions while the former of average conditions. Figure 2-1 contains plots of the atmospheric refractivity models as a function of altitude.

2.2 IONOSPHERIC INDEX OF REFRACTION

The index of refraction in the ionosphere can be expressed by the relationship

$$n = \left[1 - \left(\frac{\omega_N}{\omega}\right)^2\right]^{1/2} = \left[1 - \frac{N_e e^2}{\epsilon_o m_e \omega^2}\right]^{1/2} \tag{2-8}$$

where ω_N is the angular plasma frequency of the medium (rad/s), N_e is the electron density (electrons/m^3) e is the electron charge (1.6×10^{-19} C), m_e is the electron mass (9.1×10^{-31} kg), ϵ_o is the electric permittivity of free space ($10^{-9}/36\pi$ F/m) and ω is the angular frequency of the incident wave (rad/s).

The distribution of electron density with height is assumed to follow the Chapman model of the form

$$N_e = N_m \exp \left\{\frac{1}{2}\left[1 - \frac{h - h_m}{H_s} - \exp\left(\frac{-(h - h_m)}{H_s}\right)\right]\right\} \tag{2-9}$$

where H_s is the scale height of the neutral particles and N_m is the electron density at the level of maximum ionization, h_m.

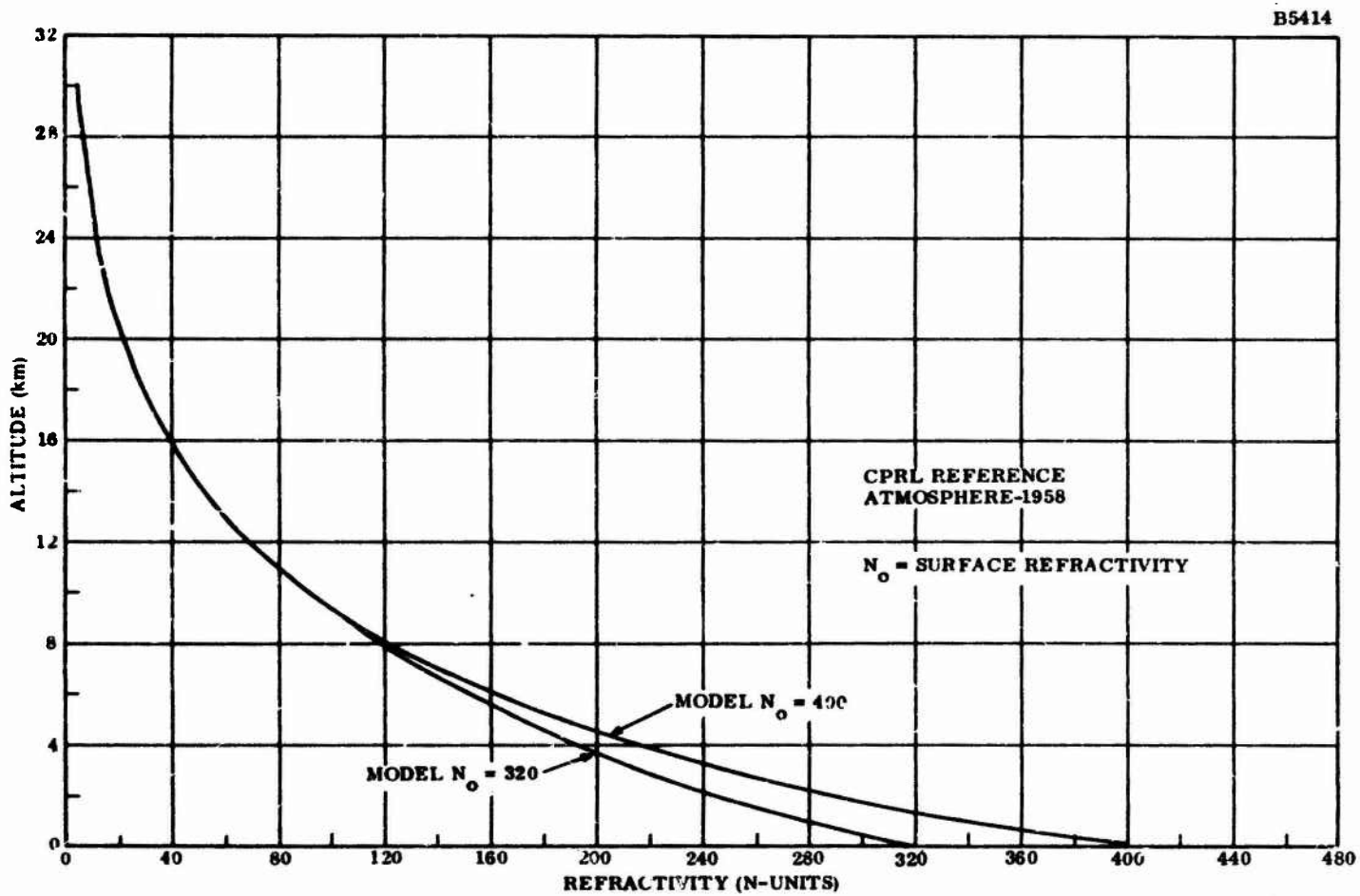

Figure 2-1. Tropospheric Refractivity As A Function of Altitude

The values of the parameters defining the electron density profiles and the equivalent plasma frequencies of the maximum ionization levels, used in the calculations, are presented in Table 2-1. The electron density levels of models B, C, and D are less than that of model A by approximately 2.7, 4.0 and 5.7 percent, respectively. It is evident that the ionization configurations are basically representative of a daytime ionosphere.

The electron density profiles of models A and D are illustrated in Figure 2-2. Minimum electron density between the E- and F1-layer is attained at 128.01 km altitude and between the F1- and F2-layer at 213.55-km altitude.

It should be noted that the ionospheric refractive index, given by Equation (2-8), is also a function of both the electron collision frequency and the earth's magnetic field.

For frequencies on the order of 10 MHz and above, and at altitudes greater than 80 km, the effect of the collision frequency term on the index of refraction is negligible (Davies, 1965).

The refractive index is slightly in error when the magnetic field is neglected. The Appleton-Hartree expression defining the index of refraction as a function of the magnetic field is discussed in Appendix A. It is found that, when the magnetic field is taken in account, the refractive index is defined by the following:

1. Longitudinal-ordinary propagation mode

$$n_{Lo} = \left\{ 1 - \frac{N_e e^2}{\epsilon_o m_e \omega^2} \left[1 + \frac{eB}{m_e \omega} \cos\theta \right]^{-1} \right\}^{1/2} \tag{2-10}$$

2. Longitudinal-extraordinary propagation mode

$$n_{Lx} = \left\{ 1 - \frac{N_e e^2}{\epsilon_o m_e \omega^2} \left[1 - \frac{eB}{m_e \omega} \cos\theta \right]^{-1} \right\}^{1/2} \tag{2-11}$$

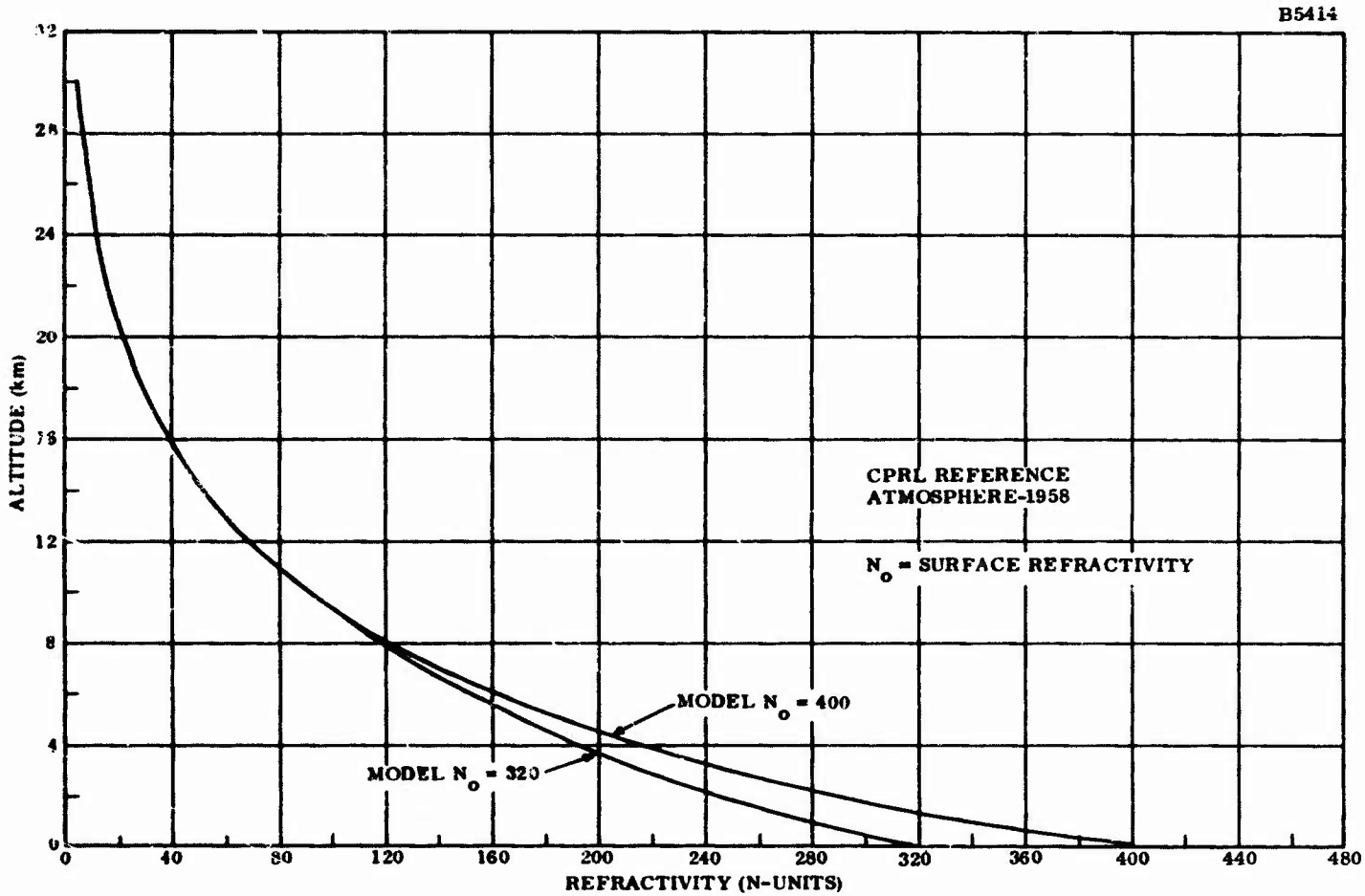

Figure 2-1. Tropospheric Refractivity As A Function of Altitude

TABLE 2-1

IONOSPHERIC ELECTRON DENSITY PROFILES

Model	Layer	Scale Height H_s (km)	Altitude (km)	Maximum Electron Density N_m (x 10^{11} electrons/m^3)	Plasma Frequency (MHz)
A	E	10	100	1.500	3.477
	F1	40	200	3.000	4.917
	F2	50	300	12.500	10.037
B	E	10	100	1.459	3.429
	F1	40	200	2.918	4.850
	F2	50	300	12.160	9.899
C	E	10	100	1.440	3.406
	F1	40	200	2.879	4.817
	F2	50	300	11.997	9.833
D	E	10	100	1.421	3.384
	F1	40	200	2.841	4.785
	F2	50	300	11.838	9.767

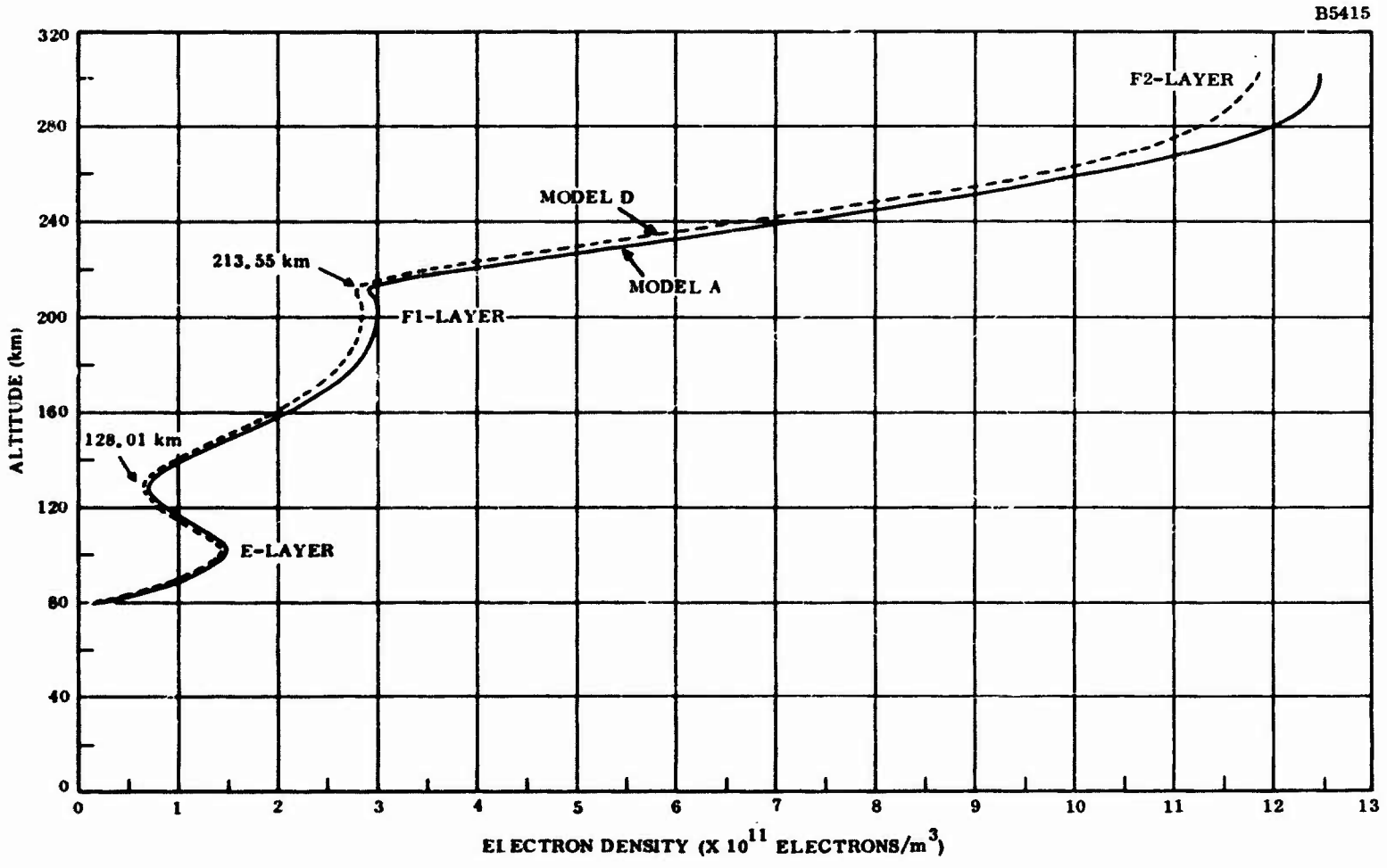

Figure 2-2. Ionospheric Electron Density As A Function of Altitude

3. Transverse-ordinary propagation mode

$$n_{To} = \left[1 - \frac{N_e e^2}{\epsilon_o m_e \omega^2} \right]^{1/2} \tag{2-12}$$

4. Transverse-extraordinary propagation mode

$$n_{Tx} = \left\{ 1 - \frac{N_e e^2}{\epsilon_o m_e \omega^2} \left[1 - \frac{N_e e^2}{\epsilon_o m_e \omega^2} \right] \left[1 - \frac{N_e e^2}{\epsilon_o m_e \omega^2} - \left(\frac{eB}{m_e \omega} \sin \theta \right)^2 \right]^{-1} \right\}^{1/2} \tag{2-13}$$

where B is the magnetic induction (Wb/m) and θ is the propagation angle, i.e., the angle between the magnetic field vector and the direction of propagation.

Table 2-2 lists the error in the refractive index for the various modes of propagation. The calculations are based on the electron density models described in Table 2-1 and on a magnetic field intensity of 0.5 G ($B = 0.5 \times 10^{-4}$ Wb/m^2) which is assumed to be invariant with altitude.

The errors are evaluated with respect to the transverse-ordinary mode of propagation which corresponds to Equation (2-8), the nonmagnetic field case. The lack of values at 10 MHz and 300-km altitude, for all modes of propagation, is due to the fact that the plasma frequency at 300 km is greater than 10 MHz, i.e., 10.037 MHz. This results in an imaginary value for the index of refraction at the 300-km level for the transverse-ordinary mode of propagation. Actually, vertical incidence reflections occur below 300 km. It is seen the maximum error in the refractive index occurs at the peak of the F2-layer and, at 30 MHz, is less than 0.4 percent. At 20 MHz, the maximum deviation increases to slightly greater than 1 percent.

TABLE 2-2

ERROR IN THE REFRACTIVE INDEX WHEN THE EARTH'S MAGNETIC FIELD IS NEGLECTED

Frequency (MHz)	Altitude (km)	Refractive Index Error (percent)			
		Propagation mode			
		Longitudinal-ordinary	Longitudinal-extraordinary	Transverse-ordinary*	Transverse extraordinary
10	100	0.84	-1.13	0	-0.16
	200	1.94	-2.63	0	-0.43
	300	-	-	-	-
20	100	0.10	-0.12	0	-0.01
	200	0.21	-0.24	0	-0.02
	300	1.09	-1.27	0	-0.11
30	100	0.03	-0.03	0	<-0.01
	200	0.06	-0.07	0	<-0.01
	300	0.38	-0.31	0	-0.02

*Nonmagnetic field case.

It should be noted that transverse propagation is applicable, to a first approximation, to transmissions originating in the midlatitudes and oriented towards the polar ionosphere. Longitudinal propagation, on the other hand, applies to midlatitudes transmissions directed equatorward. The analysis presented in this report utilized the definition of the ionospheric refractive index given by Equation (2-8).

2.3 COMPUTATIONAL PROCEDURE

In this analysis, it is assumed that (1) the troposphere is contained between the earth's surface and 30-km altitude, (2) the base of the ionosphere is located at an altitude of 80 km and (3) free space prevails in the region between the troposphere and the ionosphere.

In evaluating the effects of the tropospheric refraction phenomenon on HF propagation, the basic assumption employed is that both the troposphere and ionosphere can be considered to be stratified into m spherical layers of thickness, h_m, and constant refractive index, n_m.

The stratified layer method, although approximate in nature, can be greatly improved by merely increasing the number of layers in the medium, i.e., decreasing the thickness of each individual layer element (Millman, 1961).

The slab sizes employed in the computations are as follows: 50 m in the altitude region from h = 0 to 30 km; 50 km from h = 30 to 80 km; and 1 km from h = 80 to 300 km.

SECTION III

DISCUSSION

Estimates of the effect of tropospheric refraction on HF propagation are presented in Tables 3-1 through 3-6 which list the ground scatter distances and the true and virtual reflection heights for transmissions at 10, 20 and 30 MHz and at 1° and 3.5° elevation angles. The calculations are based on the nonmagnetic field, ionospheric index of refraction, i.e., transverse ordinary mode of propagation, defined by Equation (2-8) and apply to the four electron density models described in Table 2-1.

The analytical expressions for the true reflection height, h_r, and the virtual reflection height, h'_r, which are derived in Appendix B, are given by

$$h_r = r_o \left\{ n_o \cos E_o \left[1 - \frac{N_e e^2}{4\pi^2 \epsilon_o m_e f^2} \right]^{-1/2} - 1 \right\} \tag{3-1}$$

and

$$h'_r = r_o \left\{ \cos E_o \left(\cos \left[E_o + \frac{S}{2r_o} \right] \right)^{-1} - 1 \right\} \tag{3-2}$$

where r_o is the earth's radius, n_o is the index of refraction at the earth's surface, E_o is the apparent ground elevation angle and S is the ground scatter distance.

An examination of the data reveals that, for a given set of propagation conditions, i.e., tropospheric and ionospheric models, the true reflection height is directly proportional to the transmission frequency and to the elevation angle.

It is seen that, for a given electron density model, the true reflection height decreases with increasing surface refractivity. The ground scatter distance and the virtual reflection height, on the other hand, increase with increasing surface refractivity except in the case of the 20 MHz, 1° elevation angle data (Table 3-3) where the reverse occurs for electron density model D. This reversal can be attributed to the fact that the true height of reflection of $N_o = 0$ takes place above the peak of the F1-layer, i.e., at an altitude of 214.17 km while the $N_o = 320$ and $N_o = 400$ reflections occur below the F1-layer peak, i.e., at 181.30- and 179.56-km altitude, respectively.

TABLE 3-1

GROUND SCATTER DISTANCE AND TRUE AND VIRTUAL REFLECTION HEIGHTS FOR 10-MHz TRANSMISSIONS AT 1° ELEVATION ANGLE

Electron Density Model	Surface Refractivity (N Units)	Ground Scatter Distance (km)	Ground Scatter Distance Difference (km)	True Reflection Height (km)	True Reflection Height Difference (km)	Virtual Reflection Height (km)	Virtual Reflection Height Difference (km)
A	0	1863.96	0	81.66	0	85.38	0
	320	1949.20	85.24	81.58	-0.08	92.67	7.29
	400	1984.80	120.84	81.56	-0.10	95.80	10.42
B	0	1863.86	0	81.77	0	85.37	0
	320	1948.78	84.92	81.69	-0.09	92.63	7.26
	400	1984.26	120.40	81.66	-0.11	95.76	10.39
C	0	1863.90	0	81.82	0	85.38	0
	320	1948.70	84.80	81.74	-0.08	92.63	7.25
	400	1984.16	120.26	81.71	-0.11	95.75	10.37
D	0	1864.02	0	81.87	0	85.39	0
	320	1952.88	88.86	81.79	-0.08	92.99	7.60
	400	1984.12	120.10	81.76	-0.11	95.74	10.35

TABLE 3-2

GROUND SCATTER DISTANCE AND TRUE AND VIRTUAL REFLECTION HEIGHTS FOR 10-MHz TRANSMISSIONS AT 3.5° ELEVATION ANGLE

Electron Density Model	Surface Refractivity (N Units)	Ground Scatter Distance (km)	Ground Scatter Distance Difference (km)	True Reflection Height (km)	True Reflection Height Difference (km)	Virtual Reflection Height (km)	Virtual Reflection Height Difference (km)
A	0	1478.28	0	82.15	0	89.16	0
	320	1534.18	55.90	82.07	-0.08	94.30	5.14
	400	1559.27	80.94	82.05	-0.10	96.65	7.49
B	0	1467.92	0	82.27	0	88.23	0
	320	1507.60	39.68	82.19	-0.08	91.84	3.61
	400	1520.72	52.80	82.16	-0.11	93.05	4.82
C	0	1466.18	0	82.33	0	87.98	0
	320	1502.46	37.28	82.24	-0.09	91.37	3.39
	400	1514.52	49.34	82.22	-0.11	92.48	4.50
D	0	1463.28	0	82.39	0	87.81	0
	320	1499.74	13.46	82.30	-0.09	91.12	3.31
	400	1510.60	47.32	82.24	-0.11	92.12	4.31

TABLE 3-3

GROUND SCATTER DISTANCE AND TRUE AND VIRTUAL REFLECTION HEIGHTS FOR 20-MHz TRANSMISSIONS AT 1° ELEVATION ANGLES

Electron Density Model	Surface Refractivity (N Units)	Ground Scatter Distance (km)	Ground Scatter Distance Difference (km)	True Reflection Height (km)	True Relection Height Difference (km)	Virtual Reflection Height (km)	Virtual Reflection Height Difference (km)
A	0	4117.06	0	174.41	0	387.16	0
	320	4282.24	165.18	172.34	-2.07	418.92	31.76
	400	2535.74	-1580.32	99.96	-74.45	151.34	-235.82
B	0	4176.54	0	179.66	0	398.43	0
	320	4291.74	115.20	177.47	-2.19	420.79	22.36
	400	4297.90	121.36	176.92	-2.74	422.00	23.57
C	0	5767.26	0	214.17	0	773.97	0
	320	4609.34	-1157.92	181.30	-32.87	486.12	-287.85
	400	4360.96	-1406.30	179.56	-34.58	434.56	-339.41
D	0	5220.18	0	214.75	0	627.80	0
	320	5732.76	512.58	214.35	-0.40	764.18	136.38
	400	5934.86	714.68	214.25	-0.50	822.66	194.86

TABLE 3-4

GROUND SCATTER DISTANCE AND TRUE AND VIRTUAL REFLECTION HEIGHTS FOR 20-MHz TRANSMISSIONS AT 3.5° ELEVATION ANGLE

Electron Density Model	Surface Refractivity (N Units	Ground Scatter Distance (km)	Ground Scatter Distance Difference (km)	True Reflection Height (km)	True Reflection Height Difference (km)	Virtual Reflection Height (km)	Virtual Reflection Height Difference (km)
A	0	4590.06	0	214.49	0	597.49	0
	320	4992.12	402.04	214.12	-0.37	700.99	103.50
	400	5179.02	588.94	214.02	-0.47	752.59	155.10
B	0	4203.46	0	215.71	0	507.14	0
	320	4393.24	189.78	215.33	-0.38	550.40	43.26
	400	4453.82	250.36	215.23	-0.48	564.65	57.51
C	0	4124.14	0	216.33	0	489.67	0
	320	4224.52	100.38	215.94	-0.39	511.84	22.17
	400	4267.90	143.76	215.84	-0.49	521.60	31.93
D	0	4007.94	0	216.95	0	464.72	0
	320	4145.30	137.36	216.55	-0.40	494.30	29.58
	400	4185.52	177.58	216.45	-0.50	503.16	38.44

TABLE 3-5

GROUND SCATTER DISTANCE AND TRUE AND VIRTUAL REFLECTION HEIGHTS FOR 30-MHz TRANSMISSIONS AT 1° ELEVATION ANGLE

Electron Density Model	Surface Refractivity (N Units)	Ground Scatter Distance (km)	Ground Scatter Distance Difference (km)	True Reflection Height (km)	True Reflection Height Difference (km)	Virtual Reflection Height (km)	Virtual Reflection Height Difference (km)
A	0	3944.84	0	246.67	0	355.56	0
	320	4093.26	148.42	246.16	-0.51	382.70	27.14
	400	4185.32	240.48	246.03	-0.64	400.11	44.55
B	0	3973.60	0	248.48	0	360.73	0
	320	4045.00	71.40	247.95	-0.53	373.75	13.02
	400	4089.60	116.00	247.82	-0.66	382.01	21.28
C	0	3989.24	0	249.39	0	363.56	0
	320	4057.56	68.32	248.86	-0.53	376.07	12.51
	400	4102.84	113.60	248.72	-0.67	384.49	20.93
D	0	4011.54	0	250.38	0	367.61	0
	320	4074.66	63.12	249.77	-0.61	379.23	11.62
	400	4116.58	105.04	249.64	-0.74	387.07	19.46

TABLE 3-6

GROUND SCATTER DISTANCE AND TRUE AND VIRTUAL REFLECTION HEIGHTS FOR 30-MHz TRANSMISSIONS AT 3.5° ELEVATION ANGLE

Electron Density Model	Surface Refractivity (N Units)	Ground Scatter Distance (km)	Ground Scatter Distance Difference (km)	True Reflection Height (km)	True Reflection Height Difference (km)	Virtual Reflection Height (km)	Virtual Reflection Height Difference (km)
A	0	3472.76	0	249.44	0	359.21	0
	320	3487.48	14.72	248.94	-0.50	361.91	2.70
	400	3505.98	33.22	248.81	-0.63	365.32	6.11
B	0	3501.68	0	251.62	0	364.57	0
	320	3519.48	17.60	250.99	-0.63	367.82	3.25
	400	3538.14	36.26	250.83	-0.79	371.29	6.72
C	0	3510.42	0	252.78	0	366.14	0
	320	3550.22	39.80	252.14	-0.64	373.55	7.41
	400	3611.44	101.02	251.98	-0.80	385.10	18.96
D	0	3518.88	0	253.9[illegible]	0	367.71	0
	320	3603.22	84.34	253.30	-0.65	383.53	15.82
	400	3642.38	123.50	253.13	-0.82	391.01	23.30

It is of interest to note that the decrease in the ground scatter distance at a surface refractivity of 400-N units, electron density model A (Table 3-3) is mainly the result of the true reflection taking place at approximately the peak of the E-layer, i.e., 99.96-km altitude. This is in contrast with the $N_o = 0$ and $N_o = 320$ data which reflect at the lower portion of the F1-layer, i.e., 174.41 and 172.34 km altitude, respectively.

For 10-MHz transmissions at 1° elevation angle (Table 3-1), the differences between the different surface refractivity (N_o) computations appear to be somewhat independent of the electron density model for the three HF propagation parameters, i.e., ground scatter distance and true and virtual reflection height.

The 10-MHz, 3.5° elevation angle data (Table 3-2) and the 30-MHz data (Tables 3-5 and 3-6), however, exhibit a definite dependency in the differences between the surface refractivities with electron density model for both the ground scatter distance and the virtual reflection height.

For example, for model A which corresponds to the profile with the maximum electron density, the difference between the $N_o = 0$ and $N_o = 320$ and between the $N_o = 0$ and $N_o = 400$ ground scatter distance computations at 30 MHz, 1° elevation angle (Table 3-5) evaluate to 148.42 and 240.48 km, respectively. For model D, i.e., minimum electron density, the corresponding differences are 63.12 and 105.04 km.

A similar decrease in the differences of the ground scatter distance with electron density model is present in the 10-MHz, 3.5° electron angle data (Table 3-2). It should be noted, however, that the 30-MHz, 3.5° elevation angle calculations show the reverse effect.

An interesting disclosure in the 20-MHz results, Tables 3-3 and 3-4, is the existence of long-range propagation paths for specific tropospheric and ionospheric conditions.

It is noted that long-range propagation, i.e, ground scatter distances greater than approximately 4500 km, generally tends to occur for rays undergoing reflection at altitudes on the order of 214 km. According to Figure 2-2, this is slightly above the altitude where the F1- and F2-layer are joined together, the ionization valley being located at 213.55-km altitude.

Figures 3-1 through 3-3 disclose 20-MHz high-ray one-hop F1 mode of propagation (Pederson ray) at distances up to 6200 km, with maximum range being attained at elevation angles between approximately 1° and 3.5°. As illustrated in Figure 3-4, a slight variation in the electron density profile can result in: (1) the maximum range being acquired at the lowest elevation angle and, (2) the disappearance of the F1 propagation mode.

Long-distance one-hop F1 propagation over approximately a 4500-km path has been observed by Tveten (1961). Propagation by the one-hop F2 mode over a 5300-km path is possible according to the experimental measurements of Warren and Hagg (1958) and the theoretical calculations of Kift (1958).

Utilizing ray tracings techniques, Muldrew and Maliphant (1962) investigated the properties of long-distance, one-hop propagation. They found that long-distance propagation may occur via the F1- and as well as the F2-layer and that one-hop propagation may extend to ranges in excess of 7500 km in the temperate regions and 10,000 km in the equatorial region.

It should be apparent from Figures 3-1 through 3-4 which are visual representations of the data in Tables 3-3 and 3-4 that, at low elevation angles, the ground scatter distance is controlled to some extent by the troposphere. As previously mentioned, when tropospheric refraction is severe (i.e., high surface refractivity) the ground scatter distance is generally a maximum It is a minimum when the surface refractivity is not taken into account (i.e., $N_o = 0$). For example, the ground scatter reflection point, at 2° elevation angle for ionospheric model D, Figure 3-4, evaluates to 5052.50 km for $N_o = 400$ and decreases to 4966.34 km for $N_o = 320$ and 4738.26 km for $N_o = 0$.

At the critical (maximum) elevation angle, i.e., the angle beyond which the rays no longer undergo reflection but are transmitted through the ionosphere, the difference in the ground scatter distances is markedly reduced.

The maximum elevation angles corresponding to the propagation conditions described in Tables 3-1 through 3-6 are listed in Table 3-7. It is seen that the angle is a minimum for $N_o = 0$ and increases as N_o increases, the greatest differential between the $N_o = 0$ and the $N_o = 400$ values being achieved at the highest frequency.

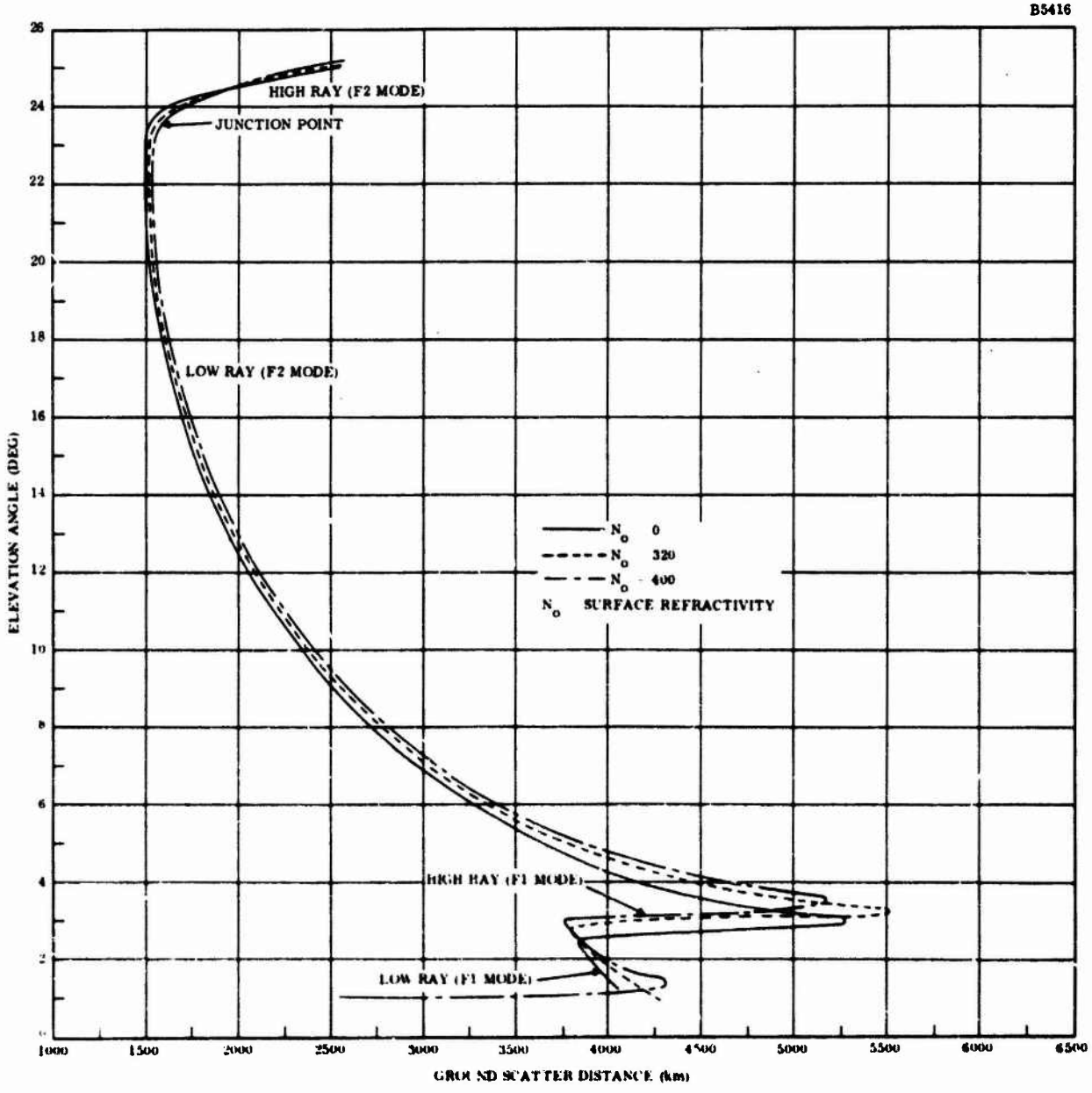

Figure 3-1. Ground Scatter Distance As A Function of Elevation Angle For Transmissions at 20 MHz, Ionospheric Electron Density Model A

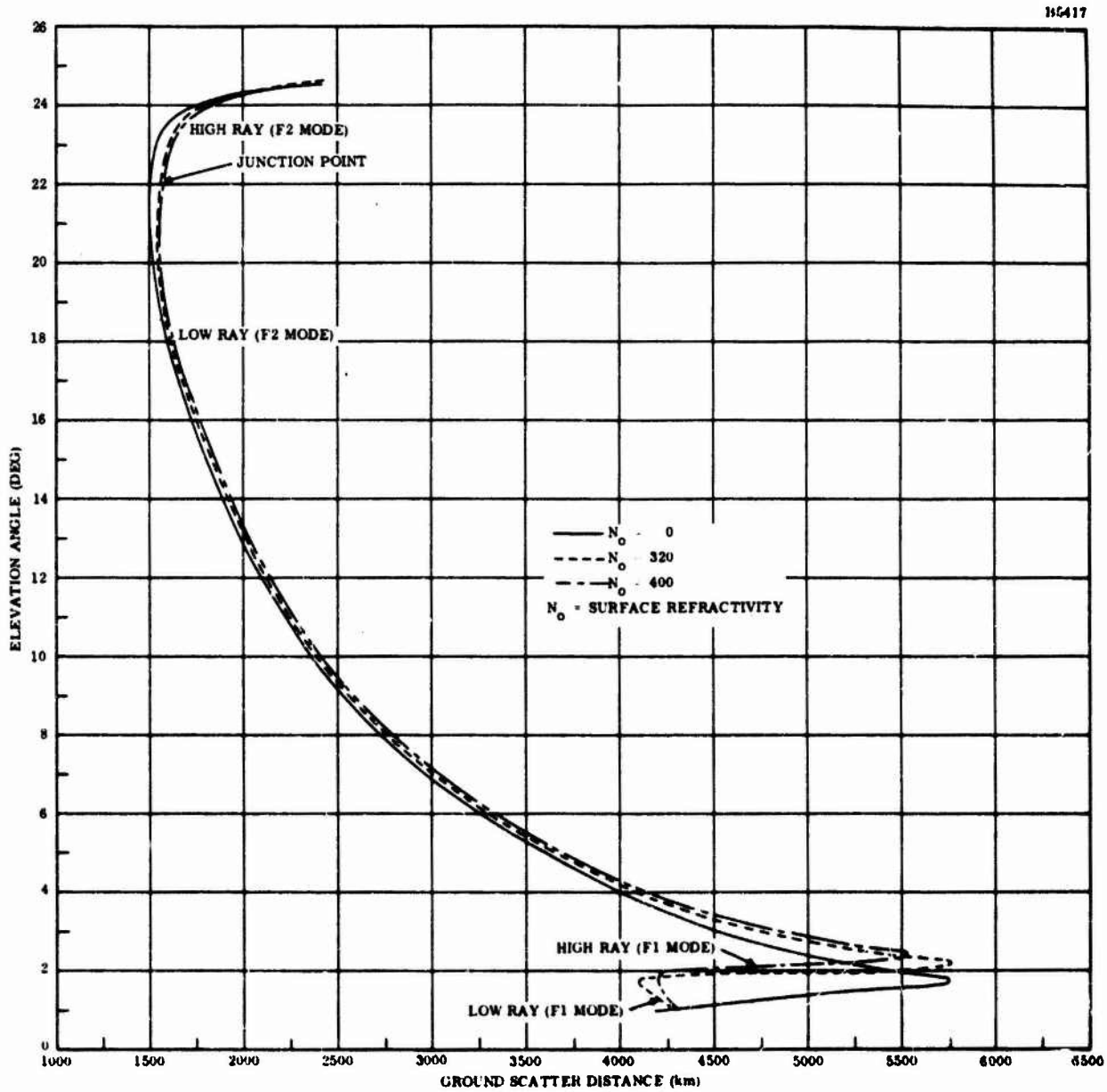

Figure 3-2. Ground Scatter Distance As A Function of Elevation Angle For Transmissions at 20 MHz, Ionospheric Electron Density Model B

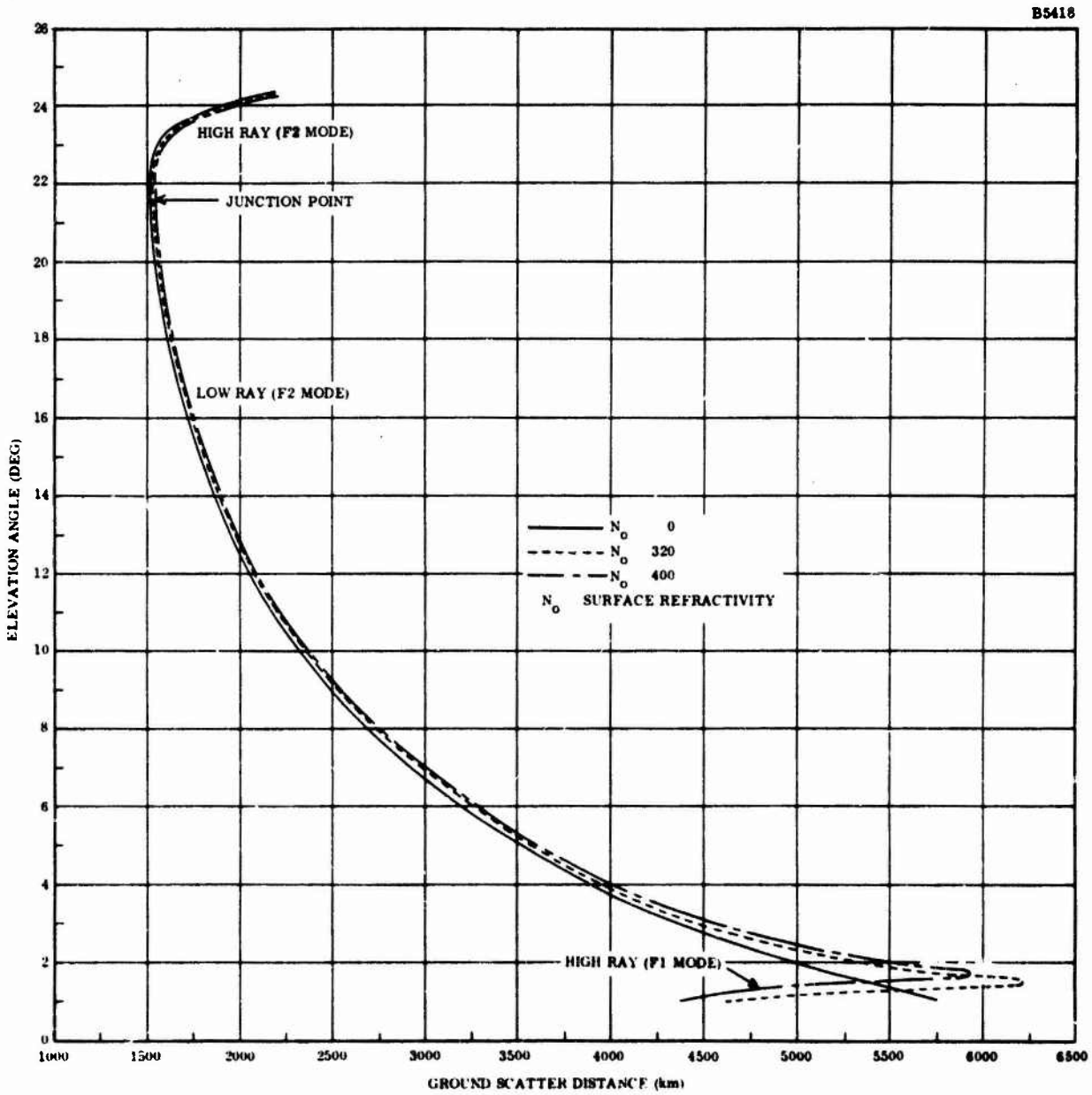

Figure 3-3. Ground Scatter Distance As A Function of Elevation Angle For Transmissions at 20 MHz, Ionospheric Electron Density Model C

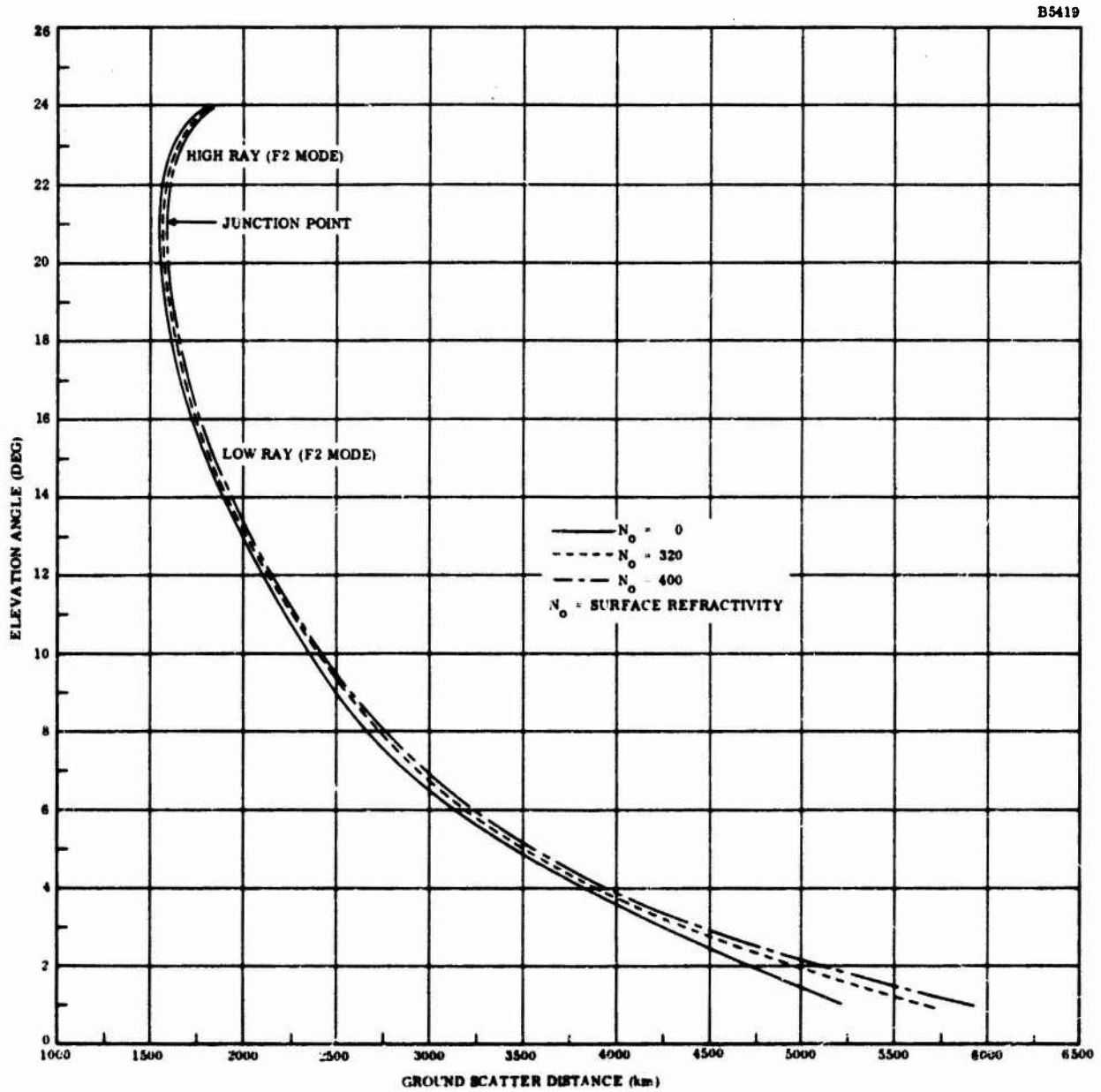

Figure 3-4. Ground Scatter Distance As A Function of Elevation Angle For Transmissions at 20 MHz, Ionospheric Electron Density Model D

TABLE 3-7

MAXIMUM ELEVATION ANGLES

Frequency (MHz)	Electron Density Model	Surface Refractivity (N Units)	Maximum Elevation Angle (Deg)
10	A	0	90°
		320	90°
		400	90°
	B	0	81.47
		320	81.47
		400	81.47
	C	0	78.99
		320	79.00
		400	79.00
	D	0	77.01
		320	77.02
		400	77.02
20	A	0	25.07
		320	25.11
		400	25.12
	B	0	24.51
		320	24.55
		400	24.56
	C	0	24.23
		320	24.27
		400	24.28
	D	0	23.96
		320	24.01
		400	24.02
30	A	0	9.63
		320	9.73
		400	9.76
	B	0	9.04
		320	9.15
		400	9.18
	C	0	8.74
		320	8.86
		400	8.89
	D	0	8.44
		320	8.56
		400	8.59

An additional feature of interest in Figures 3-1 through 3-3 is the indication of the possible existence of multiple rays incident at the same location on the earth's surface commencing at distances greater than about 3800 km. This phenomenon implies that there is a focusing of the rays which results in an apparent enhancement of the incident radiation at the long ranges.

An evaluation of HF radio focusing at maximum range caused by the ionization distribution between ionospheric layers has been made by Croft (1967).

Figures 3-5 and 3-6 are plots of the radar range, i.e., group path length, as a function of the ground scatter distance at a frequency of 20 MHz for ionospheric models A and D, respectively.

It is seen that, for a given set of propagation conditions, i.e., ionospheric model and high- or low-ray propagation mode, a linear relationship exists between the radar range and the ground scatter distance which is independent of the tropospheric refraction conditions. It follows, therefore, that there is no need to take into account the effect of refractive bending in the troposphere when determining the locationof an object in space by HF backscatter radar techniques.

On comparing Figure 3-5 with Figure 3-6, it is found that the high-ray (F2 mode) slopes are practically the same. An identical situation exists for the slopes of the low rays (F2 mode).

The presence of the low ray (F1 mode) and the high ray (F1 mode) in Figure 3-5 is consistent with the data presented in Figure 3-1.

The 30-MHz radar-range data shown in Figures 3-7 and 3-8 also display similar slopes for the low rays and for the high rays. It is noted that the slope of the data points of the high rays is slightly greater than that of the low rays for both the 20- and 30-MHz computations.

The linear relationships between the radar ranges and the ground scatter distances illustrated in Figures 3-5 through 3-8 are summarized in Table 3-8.

Additional items which should be mentioned with regard to the 30-MHz data are: (1) long-range propagation beyond 4500-km ground distance was not attainable for the four ionospheric models considered in this analysis, (2) the elevation angle versus ground scatter distance plots were similar in appearance to the curves illustrated in Figure 3-4, and (3) the ground distance traversed by the high rays tended to approach that of the low rays.

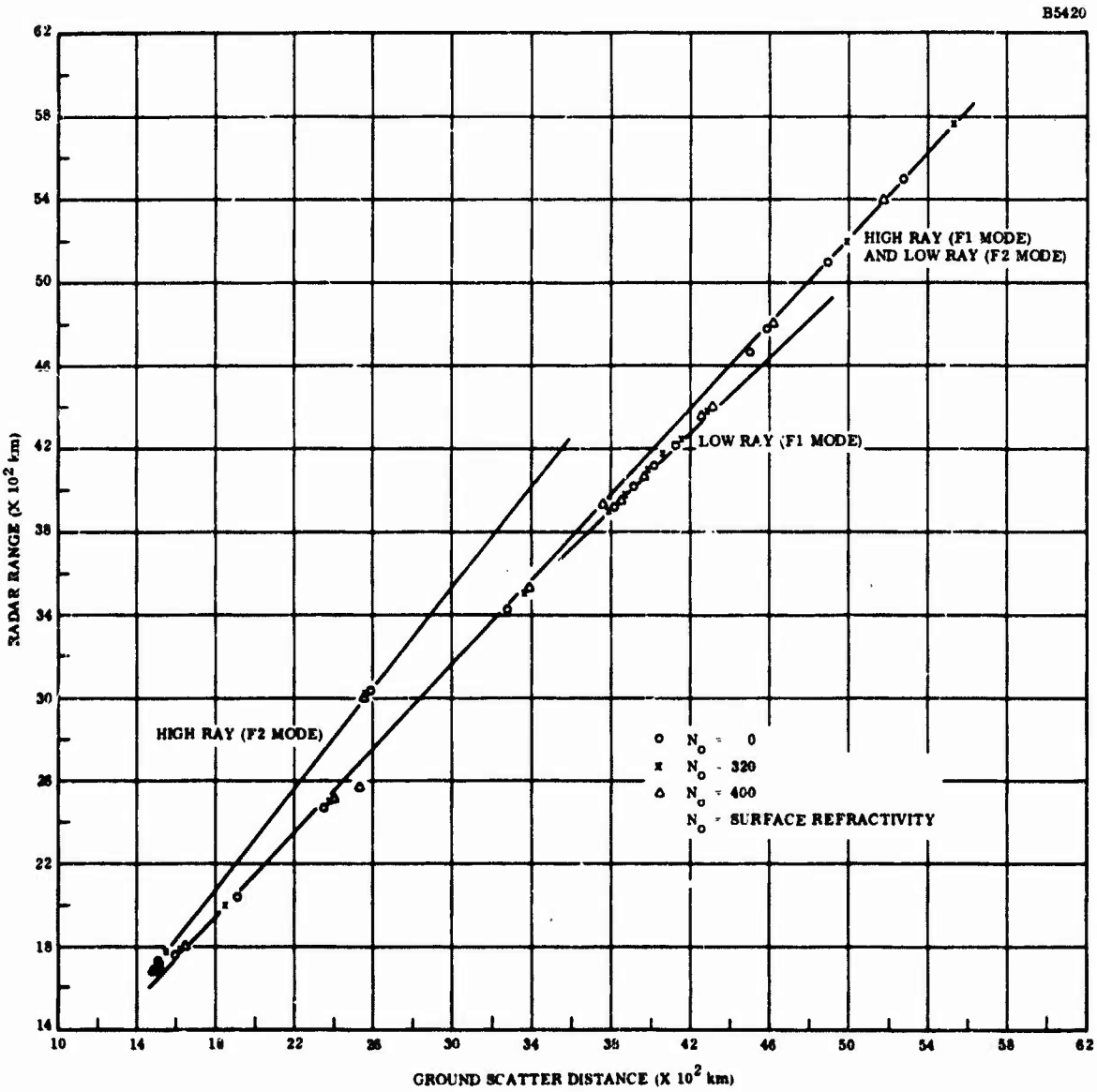

Figure 3-5. Radar Range As A Function of Ground Scatter Distance At 20 MHz For Ionospheric Electron Density Model A

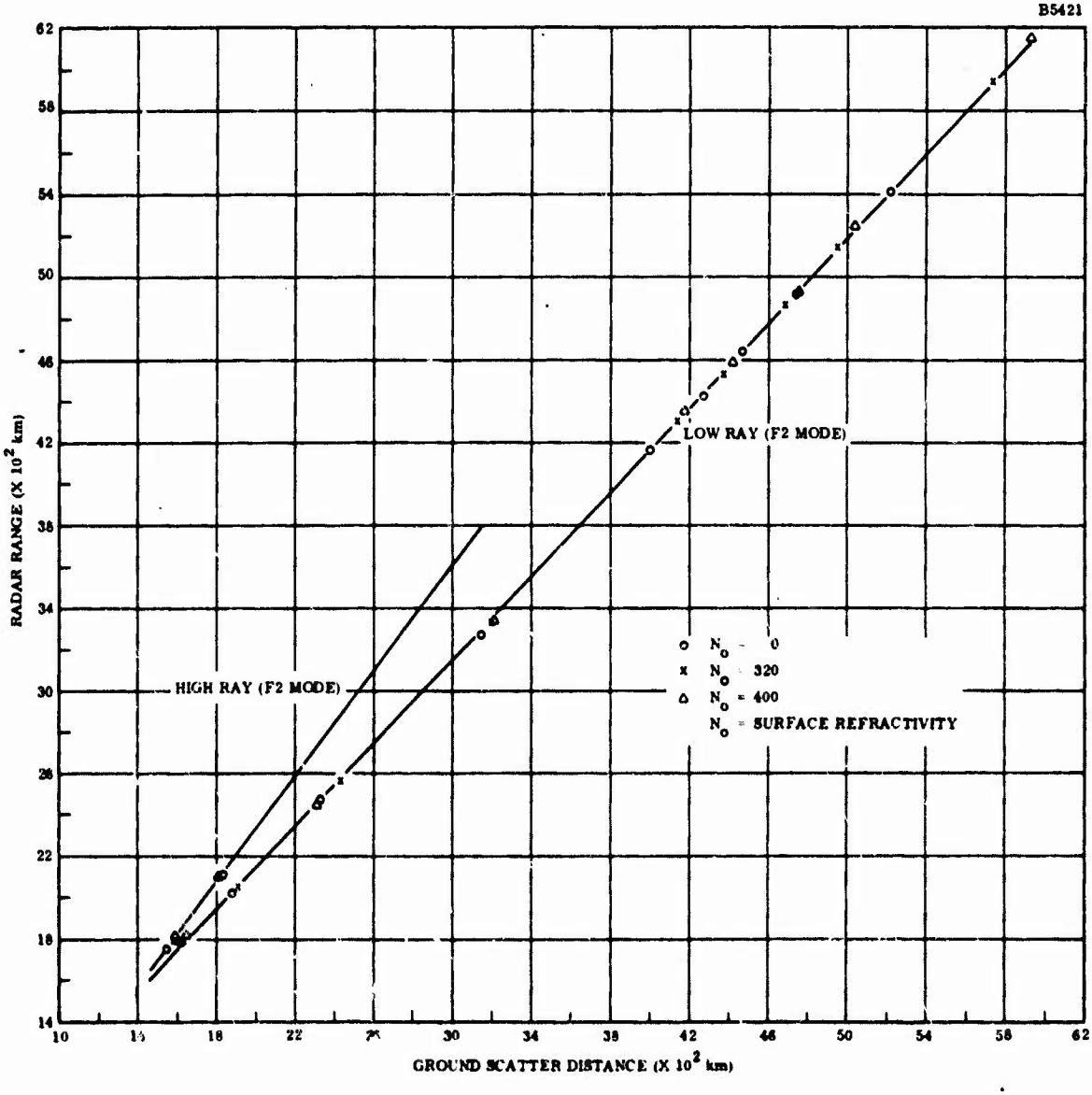

Figure 3-6. Radar Range As A Function of Ground Scatter Distance At 20 MHz For Ionospheric Electron Density Model D

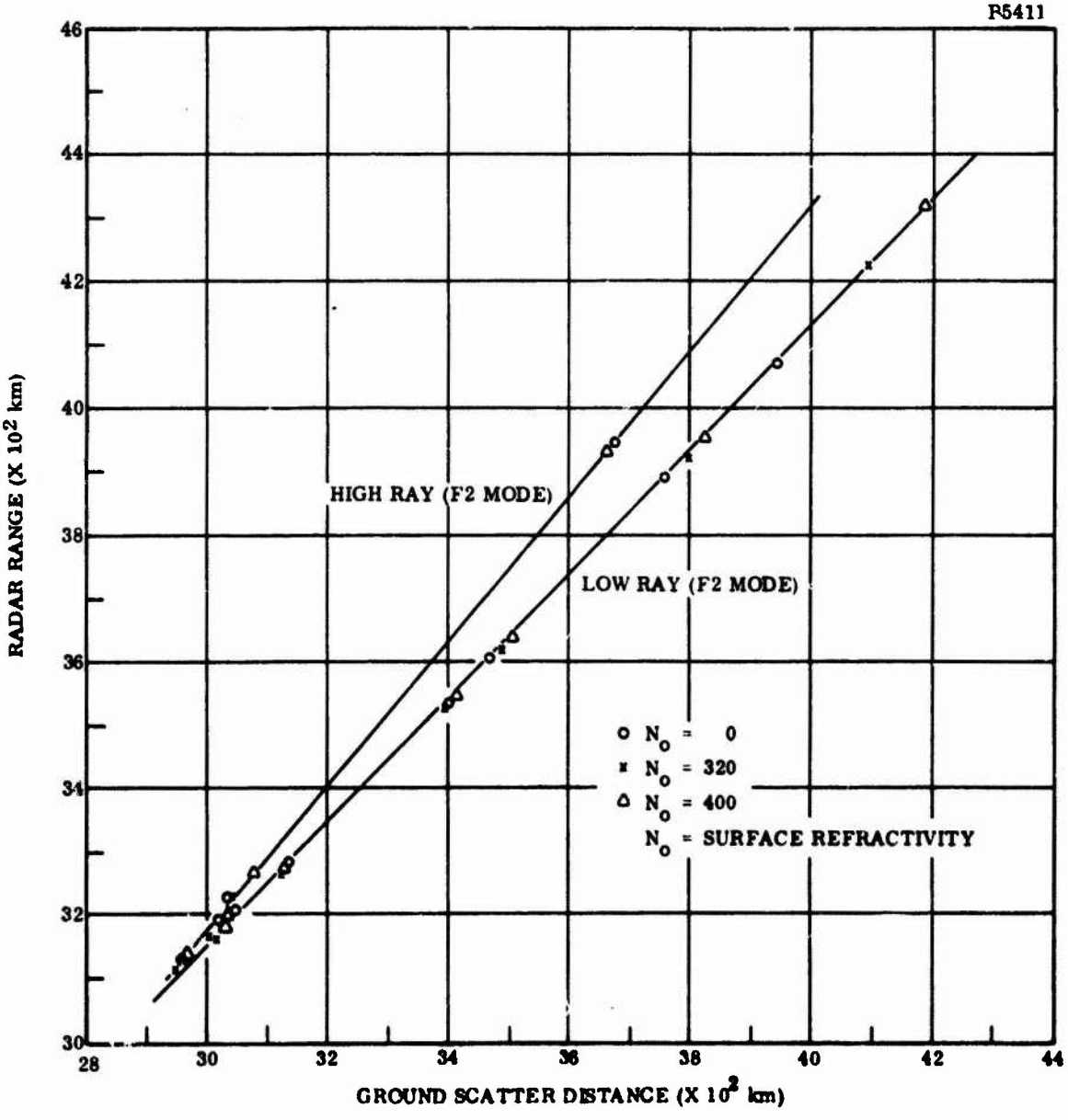

Figure 3-7. Radar Range As A Function of Ground Scatter Distance At 30 MHz For Ionospheric Electron Density Model A

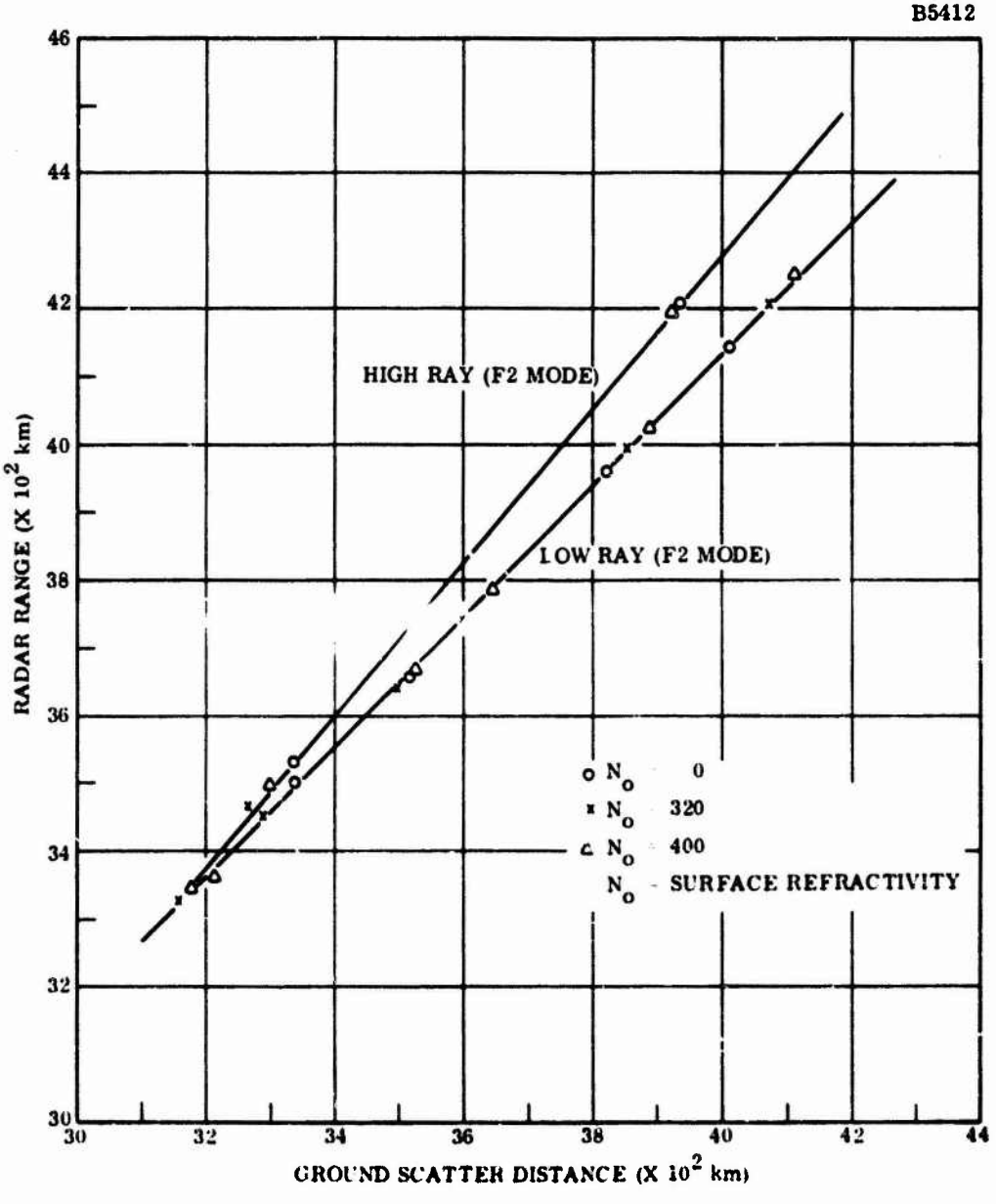

Figure 3-8. Radar Range As A Function of Ground Scatter Distance At 30 MHz For Ionospheric Electron Density Model D

TABLE 3-8

LINEAR RELATIONSHIP BETWEEN RADAR RANGE AND GROUND SCATTER DISTANCE

Frequency	Electron Density Model	Low Ray (F1 Mode)		High Ray (F1 Mode) and Low Ray (F2 Mode)		Low Ray (F2 Mode)		High Ray (F2 Mode)	
		a	b	a	b	a	b	a	b
20	A	1.06	-96.47	1.02	110.83	-	-	1.21	-103.03
	D	-	-	-	-	1.01	127.80	1.28	-240.37
30	A	-	-	-	-	0.99	165.22	1.15	-277.39
	D	-	-	-	-	0.97	245.83	1.13	-238.71

$R = aS + b$

R = Radar Range

S = Ground Scatter Distance

SECTION IV

CONCLUSIONS

The presence of tropospheric bending tends to have the following effects on HF propagation: to decrease the true height of reflection and, for the most part, to increase the surface distance over which the waves can be transmitted and to increase the virtual height of reflection.

Slight variations in the ionospheric electron density distribution could result in the ground scatter distance and virtual reflection height decreasing with increasing severity of tropospheric refraction.

Inasmuch as a linear relationship exists between the radar range, i.e., group path length, and the surface distance, tropospheric refraction effects need not be taken into account when deducing the location of a target by means of HF backscatter radar techniques.

Long distance propagation beyond 4500 km appears to occur for rays: (1) having very low takeoff angles, i.e., less than about 4° and, (2) undergoing reflection in the altitude region where the F1 and F2 layers are joined together.

It is found that, for the electron density models considered in this analysis, the long-distance propagation mode is frequency sensitive in that the extended surface coverage occurred only at 20 MHz and not at 10 and 30 MHz.

SECTION V

REFERENCES

Bean, B.R. and E.J. Dutton, "Radio Meteorology", National Bureau of Standards Monograph 92, U.S. Government Printing Office, Washington, D.C., 1966.

Croft, T.A., "HF Radio Focusing Caused by the Electron Distribution Between Ionospheric Layers", Journal of Geophysical Research, Vol. 72, pp 2343-2355, May 1, 1967.

Davies, K., "Ionospheric Radio Propagation", National Bureau of Standards Monograph 80, U.S. Government Printing Office, Washington, D.C., 1965.

Kift, F., "Single-Hop Propagation of Radio Waves to a Distance of 5300 Km", Nature, Vol. 181, pp. 1459-1460, May 24, 1958.

Millman, G.H., "Atmospheric and Extraterrestrial Effects on Radio Wave Propagation", General Electric Technical Information Series Report No. R61EMH29, June 1961.

Millman, G.H., "Tropospheric Effects on Space Communications", General Electric Technical Information Series Report No. R70EMH28, September 1970; in Tropospheric Radio Wave Propagation, AGARD Conference Proceedings No. 70, Part 1, pp (4-1) - (4-29), 1971.

Millman, G.H., "Refraction Effects on Magnetic Field Geometry and HF Propagation", Journal of Atmospheric and Terrestrial Physics, Vol. 37, pp. 751-760, May 1975.

Muldrew, D.B., and R.G. Maliphant, "Long-Distance One-Hop Ionospheric Radio-Wave Propagation", Journal of Geophysical Research, Vol. 67, pp. 1805-1815, May 1962.

Ratcliffe, J.A., "The Magneto-Ionic Theory and Its Application to the Ionosphere", Cambridge University Press, New York, 1959.

Smith, E.K., and S. Weintraub, "The Constants in the Equation for Atmospheric Refractive Index at Radio Frequencies", Proceedings of IRE, Vol. 41, pp. 1035-1037, August 1953.

Tveton, L.H., "Long-Distance One-Hop F_1 Propagation Through the Auroral Zone", Journal of Geophysical Research, Vol. 66, pp. 1683-1684, June 1961.

Warren, E. and E.L. Hagg, "Single-Hop Propagation of Radio Waves to a Distance of 5300 Km", Nature, Vol. 181, pp. 34-35, January 4, 1958.

APPENDIX A

IONOSPHERIC REFRACTIVE INDEX

The index of refraction in the ionosphere in the absence of electron collisions, i.e., absorption, is defined by (Ratcliffe, 1959)

$$n^2 = 1 - \frac{2X(1 - X)}{2(1 - X) - Y_T^2 \pm \left[Y_T^4 + 4Y_L^2(1 - X)^2\right]^{1/2}} \tag{A-1}$$

where

$$X = \left(\frac{\omega_N}{\omega}\right)^2 \tag{A-2}$$

$$Y_T = \frac{\omega_H}{\omega} \sin\theta \tag{A-3}$$

$$Y_L = \frac{\omega_H}{\omega} \cos\theta \tag{A-4}$$

and where θ is the propagation angle, i.e., the angle between the magnetic field vector and the direction of propagation, and ω is the angular frequency of the transmitted wave (rad/s).

The parameter, ω_H, is the angular gyromagnetic frequency of the electrons about the earth's magnetic field and is given by

$$\omega_H = \frac{e}{m_e} B = \frac{e}{m_e} \mu_o H \tag{A-5}$$

where e is the electron charge (1.6×10^{-19} C), m_e is the electron mass (9.1×10^{-31} kg), B is the magnetic induction (Wb/m^2), μ_o is the permeability of free space ($4\pi \times 10^{-7}$ H/m) and H is the magnetic field intensity (ampere-turns/m).

The term, ω_N, is the angular plasma frequency of the ionosphere and is given by

$$\omega_N^2 = \frac{N_e e^2}{\epsilon_o m_e} \tag{A-6}$$

where N_e is the electron density (electrons/m^3), and ϵ_o is the permittivity of free space ($10^{-9}/36\pi$ F/m).

According to Equation (A-1), there are two values for the refractive index. The positive sign is associated with the ordinary wave while the negative sign with the extraordinary wave.

The quasi-longitudinal mode of propagation can be represented by the condition

$$4Y_L^2 (1 - X)^2 >> Y_T^4 \tag{A-7}$$

Thus, for the quasi-longitudinal case, the refractive index simplifies to

$$n_L^2 = 1 - \frac{X}{1 \pm Y_L} \tag{A-8}$$

Substituting Equations (A-2) and (A-4) in this expression, it follows that

$$n_{Lo} = \left\{ 1 - \left(\frac{\omega_N}{\omega}\right)^2 \left[1 + \frac{\omega_H}{\omega} \cos\theta \right]^{-1} \right\}^{1/2} \tag{A-9}$$

$$n_{Lx} = \left\{ 1 - \left(\frac{\omega_N}{\omega}\right)^2 \left[1 - \frac{\omega_H}{\omega} \cos\theta \right]^{-1} \right\}^{1/2} \tag{A-10}$$

where the subscripts, o and x, signify the ordinary and extraordinary wave, respectively.

The condition for quasi-transverse propagation is denoted by the inequality

$$Y_T^4 >> 4Y_L^2 (1 - X)^2 \tag{A-11}$$

which is merely the reverse of Equation (A-7). For this case, Equation (A-1) reduces to

$$n_{To}^2 = 1 - X \tag{A-12}$$

$$n_{Tx}^2 = 1 - \frac{X(1 - X)}{1 - X - Y_T^2} \tag{A-13}$$

It follows from Equations (A-2) and (A-3) that

$$n_{To} = \left[1 - \left(\frac{\omega_N}{\omega}\right)^2\right]^{1/2} \tag{A-14}$$

$$n_{Tx} = \left\{1 - \left(\frac{\omega_N}{\omega}\right)^2 \left[1 - \left(\frac{\omega_N}{\omega}\right)^2\right] \left[1 - \left(\frac{\omega_N}{\omega}\right)^2 - \left(\frac{\omega_H}{\omega} \sin\theta\right)^2\right]^{-1}\right\}^{1/2} \tag{A-15}$$

It is evident that the index of refraction for the transverse-ordinary mode of propagation, Equation (A-14), is independent of the magnetic field parameters.

It is of interest to note that, when the magnetic induction (or magnetic field intensity) is assumed to be zero, Equations (A-9), (A-10), and (A-15) simplify to Equation (A-14).

APPENDIX B

HF PROPAGATION PARAMETERS

B.1 INTRODUCTION

In this appendix, the mathematical formulation of the maximum elevation angle, the maximum transmission frequency, and the true and virtual reflection heights encountered in HF propagation is described. In the derivation of the first two items, it is necessary to consider Snell's law for spherically symmetric surfaces, i.e., Bouguer's rule, which states that

$$n_o r_o \cos E_o = n_j r_j \cos E_j \tag{B-1}$$

where, as shown in Figure B-1, n_j is the refractive index at the distance, r_j, from the center of the earth to a spherical surface and E_j is the elevation angle at the distance r_j, i.e., the angle between the ray path and the tangent to the spherical surface. The zero subscript refers to the values of the parameters at the surface of the earth with r_o being the earth's radius.

The index of refraction in the troposphere is dependent on such parameters as the pressure, P, the temperature, T, and the water vapor pressure, ϵ, or, in other words,

$$n = f(P, T, \epsilon) \tag{B-2}$$

In the case of the ionosphere, the refractive index function is given by

$$n = g(N_e, f, B, \nu) \tag{B-3}$$

where N_e is electron density, f is the transmission frequency, B is the magnetic induction and ν is the electron collision frequency. In this analysis, the dependency of n on B and ν is neglected.

It is noted that, for over-the-horizon HF propagation, ionospheric reflection takes place when $E_j = 0$ in Equation (B-1).

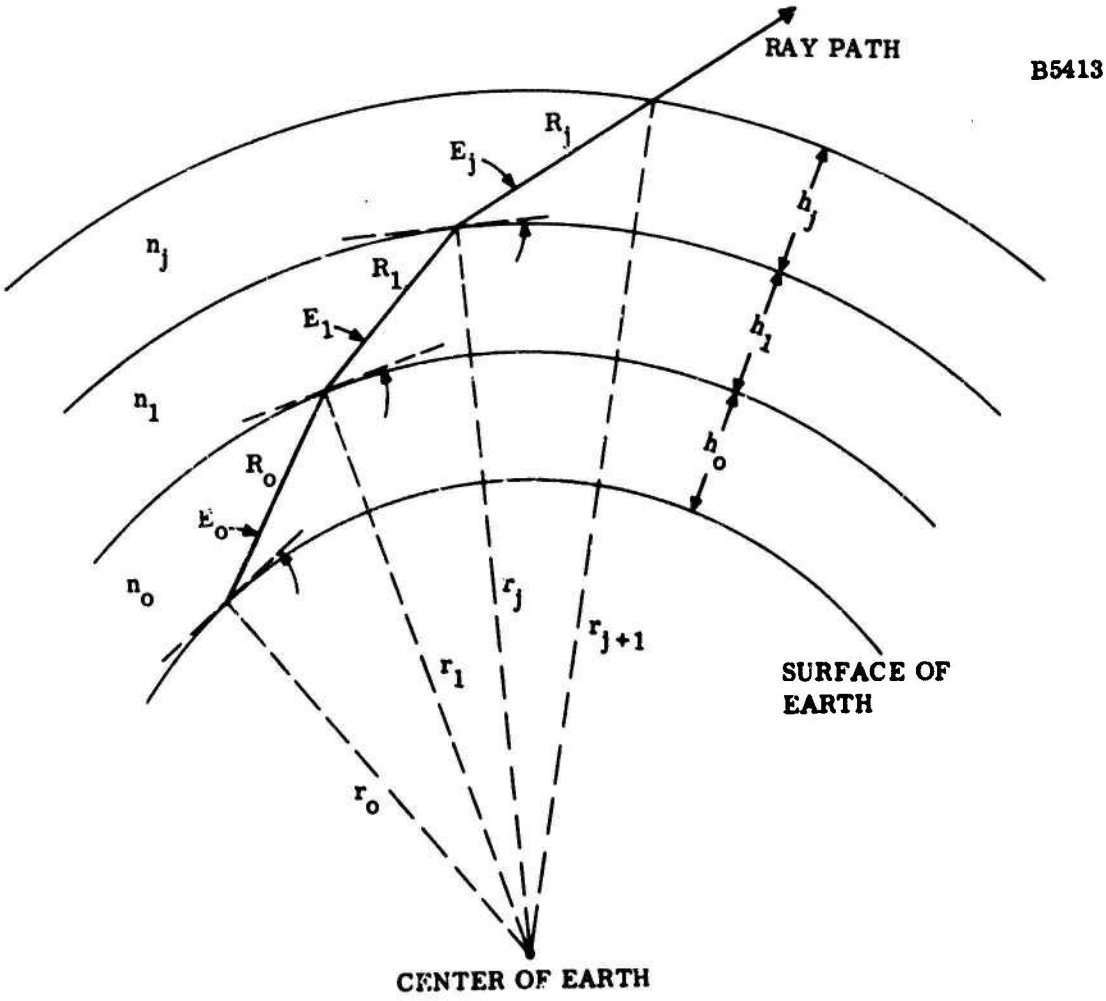

Figure B-1. Atmospheric Layer Stratification

Referring to Figure B-1, the radar range, R_r, is computed utilizing the relationship (Millman, 1961)

$$R_r = \sum_{m=0}^{j} n_m R_m + R_s + \sum_{m=0}^{j} \frac{R_m}{n_m} \qquad \text{(B-4)}$$

where the first term is the tropospheric component, the second is the free space component and the third is the ionospheric component.

B.2 MAXIMUM ELEVATION ANGLE

A typical plot of elevation angle as a function of ground scatter distance for a fixed transmission frequency is illustrated in Figure B-2. The elevation angle, E_{jun}, is the take-off angle at which propagation to the skip distance is attained and is the angle corresponding to the junction point between the low-angle ray and the high-angle ray or Pedersen ray (Davies, 1965).

To deduce the elevation angles at which high ray propagation is satisfied, it is necessary to consider Snell's law, Equation (B-1). The maximum elevation angle, E_{max}, at which transmissions can be made and still undergo ionospheric reflection is defined for the condition in which the product of n and r is a minimum. It follows that the analytical expression for this parameter is given by

$$E_{max} = \cos^{-1}\left[\frac{(nr)_{min}}{n_o r_o}\right] \qquad \text{(B-5)}$$

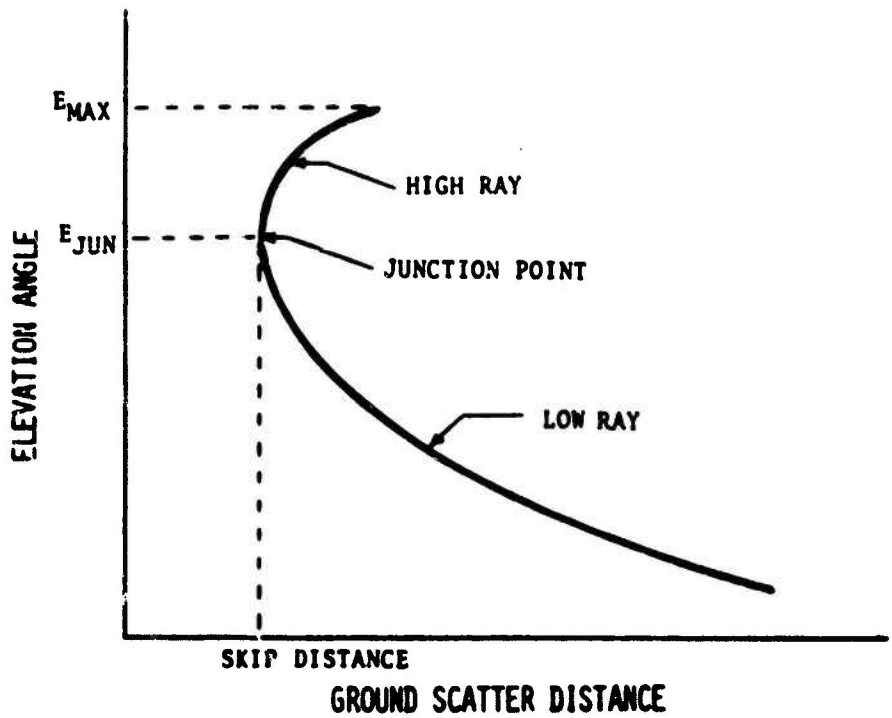

Figure B-2. Elevation Angle As A Function of Ground Scatter Distance For A Given Transmission Frequency

B.3 MAXIMUM TRANSMISSION FREQUENCY

The maximum frequency in the HF band that can encounter ionospheric reflection can be determined from Snell's law for spherically-symmetric surfaces, Equation (B-1), in conjunction with definition of the ionospheric refractive index.

For the transverse-ordinary propagation mode, i.e., the nonmagnetic field case, as given by Equation (2-8) (or Equation (2-12)), the maximum reflection frequency, f_m, can be expressed by

$$f_m = \left\{ \frac{N_m e^2}{4\pi^2 \epsilon_o m_e \left[1 - \left(\frac{n_o r_o}{r_o + h_m} \cos E_o \right)^2 \right]} \right\}^{1/2} \qquad \text{(B-6)}$$

where N_m is the maximum electron density (electrons/m^3) at the altitude, h_m, e is the electron charge (1.6×10^{-19} C), m_e is the electron mass (9.1×10^{-31} kg) and ϵ_o is the permittivity of free space ($10^{-9}/36\pi$ F/m).

It is seen that the maximum frequency for ionospheric reflection is basically a function of the maximum electron density along the propagation path, the altitude of the ionization maximum and the transmission-elevation angle.

It follows that, for ionospheric model A ($N_m = 1.25 \times 10^{12}$ electrons/m^3 and $h_m = 300$ km), as described in Table 2-1, $n_o = 1$ and $E_o = 1°$, the maximum reflection frequency evaluates to 33.798 MHz. When $n_o = 1.0004$ (surface refractivity $N_o = 400$), f_m increases to 33.939 MHz.

B.4 TRUE REFLECTION HEIGHT

An additional parameter that can be deduced from Equation (B-1) is the true ionospheric reflection height, h_r, of a transmitted signal. On combining Equation (2-8) (or Equation (2-12)) with Equation (B-1), it is found that

$$h_r = r_o \left\{ n_o \cos E_o \left[1 - \frac{N_e e^2}{4\pi^2 \epsilon_o m_e f^2} \right]^{-1/2} - 1 \right\} \qquad \text{(B-7)}$$

B.5 VIRTUAL REFLECTION HEIGHT

For an HF signal reflected obliquely from the ionosphere to a surface distance, S, the virtual (or apparent) height of reflection is the height of the equivalent linear path of the oblique signal.

As depicted in Figure B-3, the virtual reflection height, h'_r, is always greater than the true reflection height, h_r.

Utilizing the law of sines, it is seen that

$$\frac{r_o + h'_r}{r_o} = \frac{\cos E_o}{\sin \phi} \tag{B-8}$$

Since

$$\phi = \frac{\pi}{2} - \left(E_o + \frac{S}{2 r_o}\right) \tag{B-9}$$

it follows that

$$h'_r = r_o \left\{ \cos E_o \left\{ \cos \left[E_o + \frac{S}{2 r_o} \right] \right\}^{-1} - 1 \right\} \tag{B-10}$$

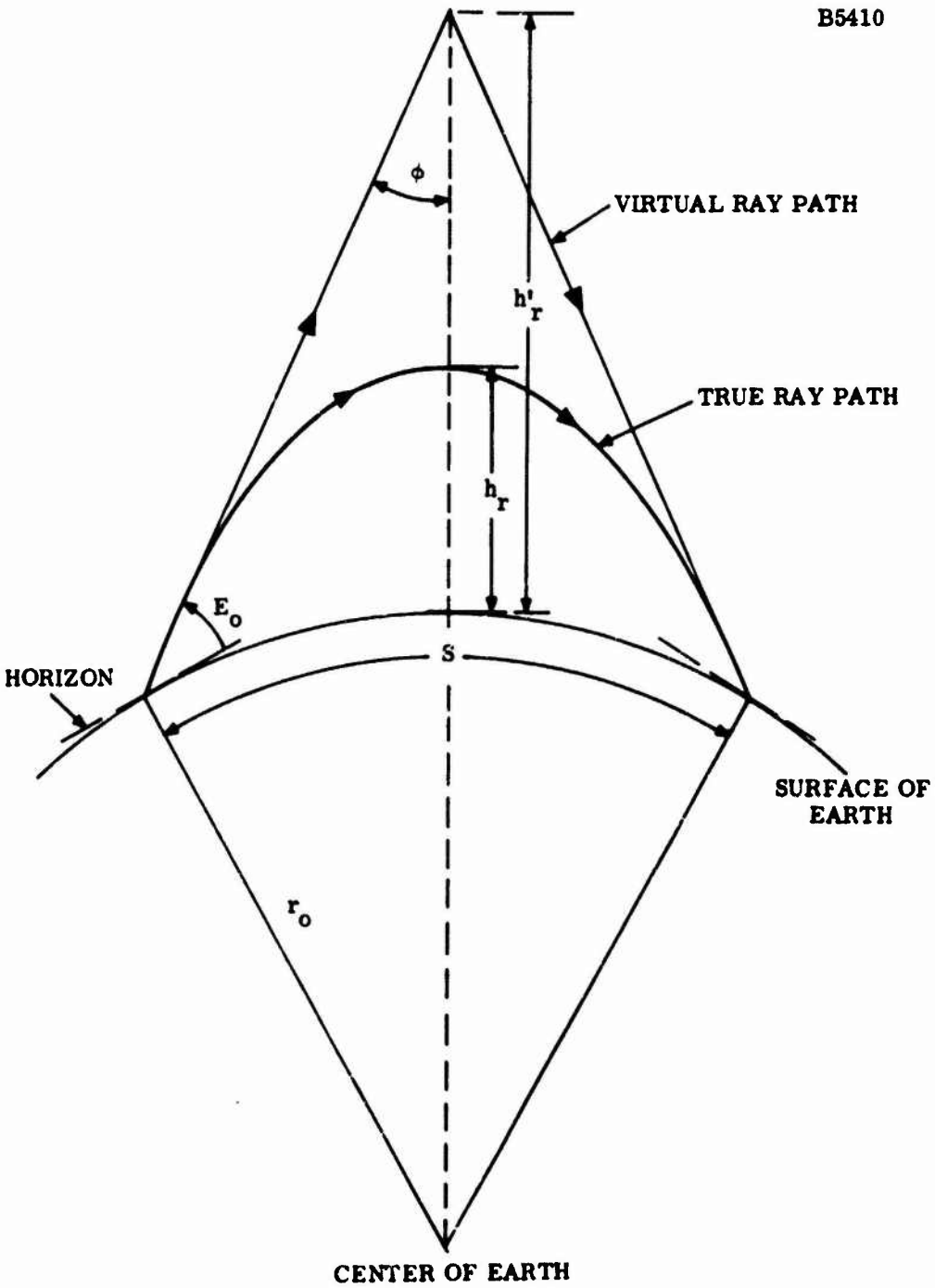

Figure B-3. True and Virtual Ray Path Geometry